J Therm Anal Calorim (2010) 99:749–754
DOI 10.1007/s10973-009-0391-y

Thermal behaviour of ammonium nitrate prills coated with limestone and dolomite powder

I. Rudjak · T. Kaljuvee · A. Trikkel · V. Mikli

MEDICTA2009 Conference

Abstract The thermal behaviour of ammonium nitrate (AN) and its prills coated with limestone and dolomite powder was studied on the basis of commercial fertilizer-grade AN and six Estonian limestone and dolomite samples. Coating of AN prills was carried out on a plate granulator and a saturated solution of AN was used as a binding agent. The mass of AN prills and coating material was calculated based on the mole ratio of AN/(CaO + MgO) = 2:1. Thermal behaviour of AN and its coated prills was studied using combined TG-DTA-FTIR equipment. The experiments were carried out under dynamic heating conditions up to 900 °C at the heating rate of 10 °C min^{-1} and for calculation of kinetic parameters, additionally, at 2, 5 and 20 °C min^{-1} in a stream of dry air. A model-free kinetic analysis approach based on the differential isoconversional method of Friedman was used to calculate the kinetic parameters. The results of TG-DTA-FTIR analyses and the variation of the value of activation energy E along the reaction progress α indicate the complex character of the decomposition of neat AN as well as of the interactions occurring at thermal treatment of AN prills coated with limestone and dolomite powder.

Keywords Coated ammonium nitrate · Dolomite · Kinetics · Limestone · TG-DTA · Thermal stability

I. Rudjak · T. Kaljuvee (✉) · A. Trikkel · V. Mikli
Department of Chemical and Materials Technology, Tallinn University of Technology, Ehitajate tee 5,
19086 Tallinn, Estonia
e-mail: tiidu@staff.ttu.ee

Introduction

Ammonium nitrate (AN) is one of the most widespread nitrogen mineral fertilizers used in the agriculture [1]. Unfortunately, thermal instability of AN, especially, if contaminated with impurities even on the low level, makes its handling and storage unpredictable which has led to several catastrophic explosions [2–4].

The thermal behaviour and the possibilities of increasing the thermal stability of AN have been studied by several authors [4–11]. Normally, solid AN follows four polymorphic phase transitions at ambient pressure—the transition $AN_{IV} \leftrightarrow AN_{III}$ occurs at 32 °C and $AN_{III} \leftrightarrow AN_{II}$ at 84 °C. In addition, a metastable transition $AN_{IV} \leftrightarrow AN_{II}$ is possible at 50 °C [10–12]. The phase transition $AN_{IV} \leftrightarrow AN_{III}$ causes drastic changes in the physical and thermodynamic properties of AN (note that $AN_{IV} \leftrightarrow AN_{II}$ does not) [12] with the following decrease in the thermal stability of AN. Therefore, avoiding the $AN_{IV} \leftrightarrow AN_{III}$ transition at manufacturing, storing and handling of AN has a great importance considering practical applications.

Another possibility to reduce the explosive potentiality of AN is to use additives which retard the decomposition of AN by increasing the reaction zone or stabilize thermal properties of AN [4, 7, 11, 13]. In [4] the influence of different reactive-grade sulphate, phosphate, and carbonate additives on the thermal stability of AN were studied. The maximum shift of the decomposition exotherm of AN towards higher temperatures was obtained with calcium carbonate additives.

Earlier, the influence of Estonian limestone and dolomite from different deposits added to AN at the mole ratio of AN/(CaO + MgO) = 2:1 on the thermal behaviour of AN was studied using combined TG-DTA-EGA (FTIR) equipment [14].

The aim of the present research was to study the thermal behaviour of AN prills coated with limestone and dolomite powder and to calculate the kinetic parameters of decomposition reactions of the coated AN prills.

Experimental

Materials

Commercial fertilizer-grade AN (34.4% N) (Tserepovetski Azot Ltd, Russia) was under investigation. Six previously ground Estonian limestone and dolomite samples (<45 μm) were used as the coating material. Coating of AN prills was carried out on a plate granulator with diameter 0.30 m using saturated solution of AN as a binding agent. The mass of AN prills and coating material was calculated on the assumption of the mole ratio of AN/(CaO + MgO) = 2:1. SEM images of the cross-sections of an AN prill and the prill coated with Anelema dolomite powder (thickness 200–300 μm) are presented in Fig. 1.

The chemical composition and specific surface area (SSA) of the limestone and dolomite samples is presented in Table 1. In limestone samples the content of total CaO and MgO was in between 52.9–54.2 mass% and 1.1–2.8 mass%, and in dolomite samples in between 26.0–29.0 mass% and 24.3–26.6 mass%, respectively. More precise characterization of the limestone and dolomite samples used has been presented in [14].

Methods

The thermal behaviour of AN and its coated prills was studied using Setaram Labsys 2000 equipment coupled to Interspec 2020 Fourier Transform Infrared Spectrometer (FTIR) by a transfer line. The experiments were carried out under dynamic heating conditions up to 900 °C at the heating rate of 10 °C min^{-1} and for calculation of kinetic parameters, additionally, at the heating rates of 2, 5 and 20 °C min^{-1} in a stream of dry air (flow rate 120 mL min^{-1}). Standard 100 μL alumina crucibles were used. A single prill was analyzed, the mass of AN prills was 15 ± 0.2 mg, the mass of coated prills varied between 24 and 26 mg.

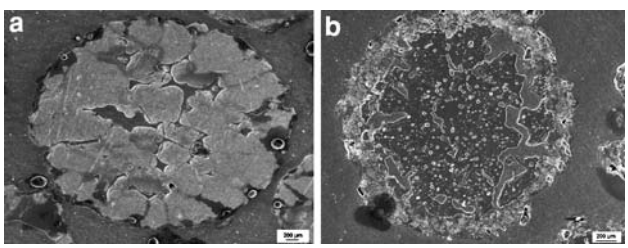

Fig. 1 SEM pictures of the cross-sections of neat AN prill (**a**) and AN prill coated with Anelema dolomite powder (**b**) (magnification ×10)

FTIR measurements were recorded in the 4,000–600 cm^{-1} region with the resolution of 4 cm^{-1} and an average out of four scans was taken. To identify the gaseous compounds, the Bio-Rad (Sadtler) KnowItAll search program and Gases and Vapours Database (code GS) were used.

The surface observations of the samples were carried out with a scanning electron microscope Jeol JSM-8404.

A model-free kinetic analysis approach based on the differential isoconversional method of Friedman [15] was used to calculate the kinetic parameters. After baseline correction and normalization, the TG signals were processed with the AKTS Advanced Thermokinetics software [16].

Results and discussion

Thermal analysis

On the DTA curves of thermally treated AN prills four endotherms between 30 and 180 °C corresponding to the respective phase transformations can be observed (Fig. 2a). Depending on the heating rate, the first, $AN_{IV} \leftrightarrow AN_{III}$ transition with a minimum on DTA curve, was fixed in a temperature interval from 52 to 71 °C. The principal transitions $AN_{III} \leftrightarrow AN_{II}$, $AN_{II} \leftrightarrow AN_{I}$ and $AN_{I} \leftrightarrow AN_{melt}$ with minimums on DTA curve occurred at temperatures from 91 to 107 °C, 131 to 150 °C and 168 to 170 °C. At higher temperatures these phase transitions were followed with a modest exoeffect and massive endoeffect with maximums and minimums on the DTA curve in between 226–258 °C and 280–324 °C, respectively, corresponding to the decomposition of AN. Besides, the endoeffect has two shoulders between 259–290 °C and 273–307 °C. The curves indicate a complicated multi-step character of the decomposition pathway of AN.

Differently, from the results with previously ground AN prills [14], when using whole prills, the temperature minimums on DTA curve for $AN_{IV} \leftrightarrow AN_{III} \leftrightarrow AN_{II} \leftrightarrow AN_{I}$ transitions were shifted at the heating rate of 10 °C min^{-1} 10–14 °C and for $AN_{I} \leftrightarrow AN_{melt}$ transition 5.2 °C towards higher temperatures, and the decomposition pathway of ground AN prills was accompanied also by a very intensive exoeffect on the DTA curve with maximum at 263 °C.

The thermograms of AN prills coated with limestone or dolomite powder showed complicated but quite similar pathway of interactions as compared to thermal behaviour of AN blends with limestone or dolomite additives at the same mole ratio of AN/(CaO + MgO)—2:1 [14]. For

Table 1 Chemical composition and specific surface area (SSA) of limestone and dolomite samples

Sample	Chemical composition/mass%[a]							BET SSA/m^2 g^{-1}
	CaO	MgO	CO_2	I. R.[b]	Al_2O_3	Fe_2O_3	$S_{sulphate}$	
Karinu	52.92	2.76	38.98	0.80	1.72	0.08	0.04	0.74
Võhmuta	53.17	1.50	39.87	1.33	1.81	0.04	0.06	1.56
Vasalemma	54.22	1.14	40.45	0.75	1.50	0.09	0.09	0.89
Kurevere	29.04	24.40	41.87	3.17	0.64	0.21	0.09	1.70
Anelema	28.85	26.63	40.81	5.83	0.84	0.14	0.10	2.44
Anelema wastes	25.95	24.29	35.58	12.41	1.41	0.37	0.10	5.79

[a] Per dry mass

[b] Insoluble residue in aqua regia

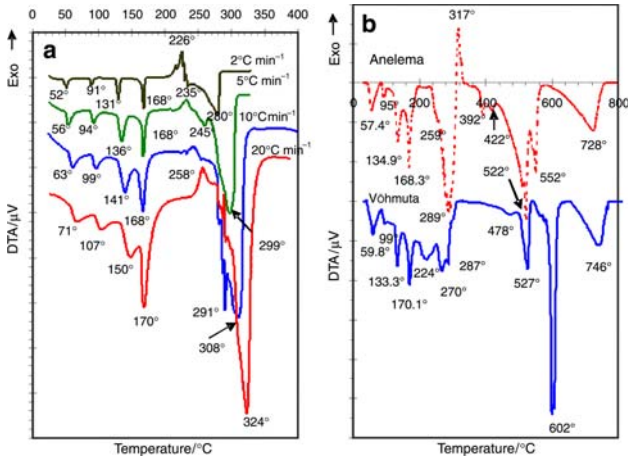

Fig. 2 DTA curves of neat AN prills at different heating rates (**a**) and AN prills coated with Anelema dolomite and Võhmuta limestone powder at the hating rate of 10 °C min^{-1} (**b**)

example, on the DTA curves of AN prills coated with Võhmuta limestone or Anelema dolomite powder, a multi-peaked endotherm was fixed in the decomposition region of AN (190–340 °C). With the prills coated with Anelema dolomite, additionally, a modest exotherm with a maximum at 317 °C was fixed (Fig. 2b). These peaks characterize the interactions between AN and Mg, Ca-carbonates with the formation of nitrates. The total mass loss at heating of the AN prills coated with Võhmuta limestone and Anelema dolomite powder up to 340 °C was 35.4 and 56.2%, respectively, indicating that dolomite ($CaCO_3{\cdot}MgCO_3$) reacts with AN less actively than limestone ($CaCO_3$).

The subsequent endotherms on the DTA curve of AN prills coated with Võhmuta limestone powder with minimums at 527 and 602 °C (Fig. 2b) characterize, respectively, the melting and decomposition of previously formed $Ca(NO_3)_2$ [17]. The double-peak endotherms on the DTA curve of AN prills coated with Anelema dolomite powder with minimums at 392 and 422 °C, and at 522 and 552 °C (Fig. 2b) characterize the decomposition of previously formed $Mg(NO_3)_2$ and $Ca(NO_3)_2$, respectively [17, 18]. The last endotherms on DTA curves with minimums at 746 and 728 °C (Fig. 2b), describe the decomposition of residual carbonates.

The total mass loss at heating of the AN prills coated with Võhmuta limestone powder up to 610 and 770 °C was 65.1 and 71.7% and in the case of Anelema dolomite powder coating when heated up to 440, 560 and 770 °C, respectively, 59.1, 71.0 and 79.3%.

FTIR analysis

FTIR spectra of gaseous compounds evolved at thermal treatment of neat AN prills showed peaks characteristic to NH_3 (967 and 932 cm^{-1}), N_2O (2,235 and 2,215 cm^{-1}), NO_2 (1,630 and 1,595 cm^{-1}) and H_2O (bands in the broad ranges 3,900–3,500 and 1,900–1,300 cm^{-1}) having maximum intensity at 250, 280, 300 and 300 °C, respectively (Fig. 3a). The peaks characteristic to NO_2 and NH_3 were 1.5–2 times more intensive as compared to these obtained at thermal treatment of previously ground AN prills [14]. It is in a good correlation with the results presented in [19, 20]—the decomposition of AN, after dissociation into NH_3 and HNO_3 in the first step, can follow different pathways with the formation of N_2O at lower temperatures (<280 °C) and NO_2 at higher temperatures. Compactable AN prills follow preferably high-temperature route of AN decomposition. So, the decomposition pathway of AN at thermal treatment could be presented by the following simplified equations:

$$NH_4NO_3 \rightarrow NH_3 + HNO_3 \quad (1)$$

$$NH_4NO_3 \rightarrow N_2O + 2H_2O \quad (2)$$

$$2HNO_3 \rightarrow H_2O + 2NO_2 + {}^1/_2O_2 \quad (3)$$

In the FTIR spectra of AN prills coated with limestone powder, the peaks characteristic to NH_3 and CO_2 (2,358 and 2,354 cm^{-1}) dominated in the temperature interval from 200 to 300 °C. The characteristic peaks for H_2O, NO_2 and N_2O were also present, but had lower intensity

(Fig. 3b). In the FTIR spectra of AN prills coated with dolomite powder, the peaks characteristic to NO_2 and, especially, to N_2O in the same temperature interval were presented more intensively (Fig. 3c). This indicates that at these temperatures the following interaction between AN and $CaCO_3$ with the formation of $Ca(NO_3)_2$ dominated:

$$2\ NH_4NO_3 + CaCO_3 \rightarrow Ca(NO_3)_2 + 2\ NH_3 + CO_2 + H_2O \quad (4)$$

The reaction of AN with $MgCO_3$

$$2\ NH_4NO_3 + MgCO_3 \rightarrow Mg(NO_3)_2 + 2\ NH_3 + CO_2 + H_2O \quad (5)$$

was not as complete as $MgCO_3$ is thermodynamically less reactive towards AN than $CaCO_3$. In addition, using dolomite as the coating material, more AN decomposed with the formation of nitrous gases as compared to limestone coating. Corresponding tendencies in FTIR spectra collected in the same temperature interval at thermal treatment of AN blends with limestone and dolomite additives were observed also in [14].

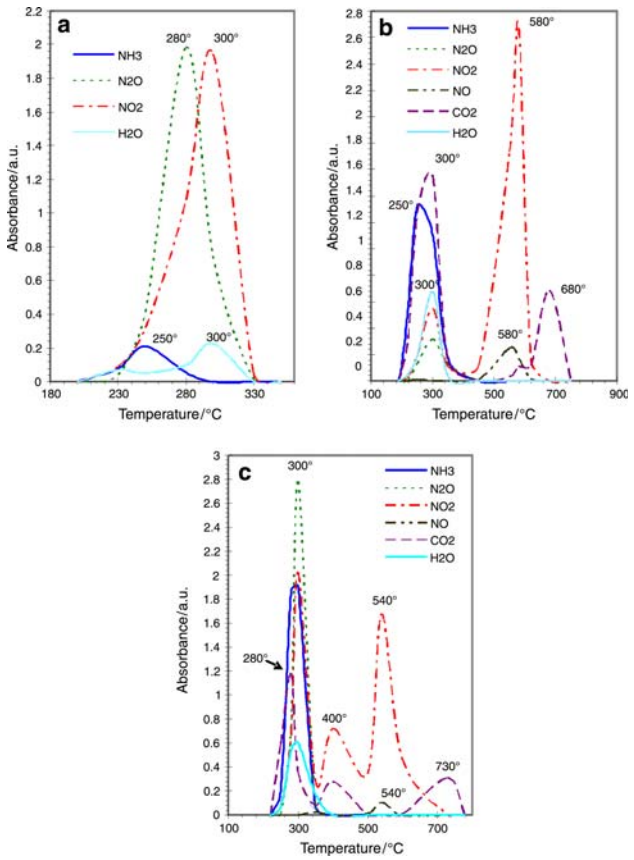

Fig. 3 Absorbance profiles of gaseous compounds evolved at thermal treatment of neat AN prill (**a**), AN prills coated with Võhmuta limestone (**b**) and Anelema dolomite (**c**) powder at the heating rate of 10 °C min^{-1}

The second maximum on the absorbance profile of CO_2 at 390–400 °C at thermal treatment of AN prills coated with Anelema dolomite powder (Fig. 3c) points to the partial interaction of formed $Mg(NO_3)_2$ with $CaCO_3$:

$$Mg(NO_3)_2 + CaCO_3 \rightarrow Ca(NO_3)_2 + MgO + CO_2 \quad (6)$$

The peaks characteristic to NO_2 were fixed in FTIR spectra once again with maximum intensities at 400 and 540 °C when using Anelema dolomite coating (Fig. 3c) and with maximum intensity at 580 °C when using Võhmuta limestone coating (Fig. 3b). These are the temperatures of decomposition of Mg, Ca-nitrates formed at lower temperatures. The bands with maximum intensity at 540 °C when using dolomite and at 580 °C in the case of limestone, fixed in FTIR spectra in the 1,800–1,950 cm^{-1} region, also indicate the formation and emission of NO (Fig. 3b, c). The decomposition of Mg, Ca-nitrates can be presented by the following simplified equations:

$$Mg(NO_3)_2 \rightarrow MgO + NO_2 + NO + O_2 \quad (7)$$

$$Ca(NO_3)_2 \rightarrow CaO + NO_2 + NO + O_2 \quad (8)$$

The last maximum on the absorbance profile of CO_2 at 680 and 730 °C obtained at thermal treatment of AN prills coated, respectively, with Võhmuta limestone (Fig. 3b) and Anelema dolomite powder (Fig. 3c), is caused by the decomposition of residual carbonates:

$$MgCO_3 \cdot CaCO_3 \rightarrow MgO + CaCO_3 + CO_2 \quad (9)$$

$$CaCO_3 \rightarrow CaO + CO_2 \quad (10)$$

Hereby, the results of EGA from the experiments with coated AN prills confirmed that the interactions between AN and carbonates contained in the coating materials used proceeded mostly by similar pathway as compared to AN blends with limestone and dolomite [14]—partially, or almost completely through the formation of $Mg(NO_3)_2$ and $Ca(NO_3)_2$ which decomposed thereupon in the temperature range of 360–620 °C.

Determination of kinetic parameters

The reaction rates and the kinetic parameters *A* and *E* for the decomposition of AN prills calculated using the differential isoconversional method of Friedman are presented in Fig. 4, and for AN prills coated with limestone or dolomite powder in Table 2. Here, step I presents data for low temperature region (depending on the heating rate between 150 and 350 °C) where interactions between AN and carbonates with the formation of Ca, Mg-nitrates take

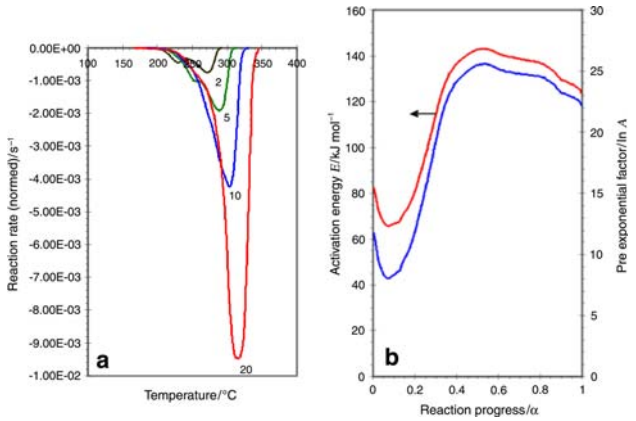

Fig. 4 Reaction rate $d\alpha/dt$ (DTG, normalized signals) as a function of the temperature for different heating rates (**a**), and activation energy E_a and pre-exponential factor A determined by Friedman analysis as a function of the reaction progress (**b**) for the decomposition of neat AN prills. (The value of the heating rate in °C min^{-1} are marked on the curves.)

place, but also unreacted AN, especially, in the case of dolomite coating decomposes. Step IIA presents data characterizing reactions occurring with $Mg(NO_3)_2$ in the temperature region from 310 to 450 °C and step IIB data characterizing decomposition of $Ca(NO_3)_2$ in the temperature region of 420–620 °C. For AN prills coated with limestone powder having poor content of MgO (Table 1) the step IIA is missing.

For neat AN prills the activation energy in the range of conversion (decomposition) level $0.1 < \alpha < 0.9$ was in between 66.7 and 142.7 kJ $mole^{-1}$ (pre-exponential factor A from 4.0×10^3 to 1.2×10^{11} s^{-1}) (Fig. 4b) varying at that more than this calculated in [14] in the case of powdered neat AN (E between 92.7 and 106.8 kJ $mole^{-1}$) indicating more complicated character of decomposition of AN in prills than in powdered form.

For AN prills coated with limestone and dolomite powder the value of activation energy in the same range of α (decomposition and interactions of AN with carbonates—step I) varied also in a wide range. For example, for AN prills coated with Võhmuta limestone powder from 82.8 to 119.6 kJ $mole^{-1}$ (pre-exponential factor A in between 7.3×10^5 and 1.3×10^{10} s^{-1}), with Kurevere dolomite powder from 111.3 to 154.8 kJ $mole^{-1}$ (A in between 2.0×10^8 and 2.9×10^{12} s^{-1}). For step IIA (interactions with Mg-nitrate) and IIB (decomposition of Ca-nitrate) the value of activation energy also varied in a great extent. For example, for AN prills coated with Kurevere dolomite powder from 185.2 to 344.7 kJ $mole^{-1}$ (A in between 1.3×10^{12} and 2.8×10^{24} s^{-1}) during step IIA and from 154.6 to 194.1 kJ $mole^{-1}$ (A in between 5.9×10^7 and

Table 2 The activation energy E (kJ $mole^{-1}$) and pre-exponent factor ln A versus reaction progress α

Sample	α																	
	0.1		0.2		0.3		0.4		0.5		0.6		0.7		0.8		0.9	
	E	ln A	E	ln A	E	ln A	E	ln A	E	ln A	E	ln A	E	ln A	E	ln A	E	ln A
Step I:																		
Neat AN	66.7	8.3	81.0	11.9	114.4	19.3	136.7	24.2	142.7	25.5	141.0	25.2	138.7	24.8	138.7	24.5	129.6	23.2
AN + Võhmuta	119.6	23.3	114.4	21.7	110.9	20.5	106.5	19.3	104.6	18.6	101.1	17.7	95.1	16.3	87.2	14.4	82.8	13.5
AN + Karinu	106.7	20.0	90.7	20.6	96.0	14.5	83.9	13.8	81.7	13.2	79.0	12.5	80.2	12.8	83.6	13.5	87.6	14.4
AN + Vasalemma	109.7	19.3	91.9	15.2	85.5	13.6	85.8	13.6	92.2	14.9	106.8	17.9	116.3	19.9	119.2	20.5	118.7	20.4
AN + Kurevere	111.3	19.1	118.8	20.9	131.5	23.7	154.8	28.7	153.3	28.2	152.6	28.0	144.9	26.2	133.9	23.8	131.4	23.2
AN + Anelema	107.2	18.1	101.5	16.9	97.9	16.1	97.9	16.2	97.9	16.2	99.6	16.6	101.7	17.1	103.9	17.5	107.2	18.2
AN + Anelema wastes	92.4	15.0	95.6	15.9	100.0	16.9	102.6	17.5	101.7	17.4	103.0	17.6	102.0	17.4	102.3	17.5	101.9	17.4
Step II:																		
AN + Võhmuta	124.8	11.6	120.4	10.7	206.9	23.5	247.0	29.5	255.3	30.8	230.2	27.5	223.7	26.8	219.9	26.4	206.6	24.7
AN + Karinu	170.3	17.9	205.1	23.1	200.8	22.6	170.0	18.4	156.6	16.7	173.1	19.3	178.3	20.2	182.8	21.0	191.3	22.4
AN + Vasalemma	192.8	22.3	194.0	22.3	192.1	21.7	197.0	22.3	219.5	25.9	229.6	27.7	218.0	26.3	223.5	27.2	228.1	28.1
AN + Kurevere, IIA	253.8	40.0	335.5	54.8	344.7	56.3	308.2	49.7	265.7	42.0	234.9	36.5	219.1	33.6	205.3	31.3	185.2	27.9
AN + Kurevere, IIB	160.3	18.7	154.6	18.0	158.9	18.9	165.4	19.8	169.0	20.3	168.1	20.0	155.9	17.9	172.1	20.3	194.1	23.8
AN + Anelema, IIA	246.1	39.3	292.5	47.7	321.1	52.8	316.3	51.9	297.4	48.4	285.7	46.2	283.4	17.9	172.1	20.3	194.1	23.8
AN + Anelema, IIB	177.4	20.9	153.8	17.3	145.8	16.3	164.8	19.3	175.0	20.9	174.2	20.6	163.0	18.8	123.6	12.9	135.5	14.9
AN + Anelema wastes, IIA	253.8	41.0	299.2	49.4	110.1	51.3	304.0	50.1	287.7	47.1	273.0	44.5	263.9	42.8	249.2	40.1	228.4	36.4
AN + Anelema wastes, IIB	160.3	18.7	154.6	18.0	158.9	18.8	165.4	19.3	169.0	20.3	168.1	20.0	155.9	17.9	172.1	20.3	194.1	23.8

2.2×10^{10} s^{-1}) during step IIB (Table 2). For AN prills coated with Võhmuta limestone powder the activation energy for step II varied from 120.4 to 255.3 kJ $mole^{-1}$ (*A* in between 4.4×10^4 and 2.4×10^{13} s^{-1}).

The results obtained indicate the complex character of the decomposition of AN and the interactions occurring in the AN prills coated with limestone or dolomite powder, prove the formation (step I) and decomposition of nitrates (step II), and point to the visible dependence of the values of activation energy and pre-exponential factor on the reaction extent.

Conclusions

AN prills coated with limestone or dolomite powder follow at thermal treatment predominantly the same complicated but safe behaviour as AN blends with limestone or dolomite additives—interactions between AN and Ca, Mg-carbonates with the formation of Ca, Mg-nitrates excluding exothermic explosive decomposition of AN and the following decomposition of the formed nitrates at higher temperatures.

Acknowledgements This work was partly supported by the Estonian Ministry of Education and Research (SF0140082s08) and the Estonian Science Foundation (G7548).

References

1. International Fertilizer Industry Association's Public Statistics 2009. Fertilizer supply statistics. http://www.fertilizer.org/ifa/statistics.asp.
2. Keeping faith with AN. Fertil Int. 2004;401 July/August:6–9.
3. Dechy N, Bourdeaux T, Ayrault N, Kordek M-A, Le Coze J-C. First lessons of the Toulouse ammonium nitrate disaster, 21st September 2001, AZF plant, France. J Hazard Mater. 2004; 111:131–8.
4. Oxley JC, Smith JL, Rogers E, Yu M. Ammonium nitrate: thermal stability and explosivity modifiers. Thermochim Acta. 2002;384:23–45.
5. Olszak-Humienik M. On the thermal stability of some ammonium salts. Thermochim Acta. 2001;378:107–12.
6. Sun J, Sun Z, Wang Q, Ding H, Wang T, Jiang C. Catalitic effects of inorganic acids on the decomposition of ammonium nitrate. J Hazard Mater. 2005;127:204–10.
7. Remya Sudhakar AO, Mathew F. Thermal behaviour of CuO doped phase-stabilised ammonium nitrate. Thermochim Acta. 2006;451:5–9.
8. Wu HB, Chan CK. Effects of potassium nitrate on the solid phase transitions of ammonium nitrate particles. Atm Environ. 2008;42:313–22.
9. Skordilis CS, Pomonis PJ. The influence of Mn, Co and Cu cations on the thermal decomposition of NH_4NO_3 in pure form and supported on alumina. Thermochim Acta. 1993;216:137–46.
10. Kestilä E, Harju MEE, Valkonen J. Differential scanning calorimetric and Raman studies of phase transition V - IV of ammonium nitrate. Thermochim Acta. 1993;214:67–70.
11. Simões PN, Pedroso LM, Portugal AA, Campos JL. Study of the decomposition of phase stabilized ammonium nitrate (PSAN) by simultaneous thermal analysis: determination of kinetic parameters. Thermochim Acta. 1998;319:55–65.
12. Laurent B. Straight ammonium nitrate fertilizer granule-prill stabilization: theoretical possibilities. Proceedings of the International Industry Association Technical Conference, Chennai, India. http://www.fertilizer.org/ifa/Library/Conference proceedings/Technical conferences/2002_tech_laurent.pdf.
13. Lang AJ, Vyazovkin S. Phase and thermal stabilization of ammonium nitrate in the form of PVP-AN glass. Mater Lett. 2008;62:1757–60.
14. Kaljuvee T, Edro E, Kuusik R. Influence of lime-containing additives on the thermal behaviour of ammonium nitrate. J Therm Anal Calorim. 2008;92:215–21.
15. Friedman HL. Kinetics of thermal degradation of char-forming plastics from thermogravimetry. Application to a phenolic plastic. J Polym Sci. 1965;6C:183–95.
16. AKTS Software and SETARAM Instruments: a global solution for kinetic analysis and determination of the thermal stability of materials. Switzerland: AKTS AG; 2006. p. 88.
17. Madarász J, Varga PP, Pokol G. Evolved gas analyses (TG/DTA-MS and TG-FTIR) on dehydration and pyrolysis of magnesium nitrate hexahydrate in air and nitrogen. J Anal Appl Pyrolysis. 2007;79:475–8.
18. Ettarh C, Galwey AK. A kinetic and mechanistic study of the thermal decomposition of calcium nitrate. Thermochim Acta. 1996;93:203–19.
19. Brower KR, Oxley JC, Tewari M. Evidence for homolytic decomposition of ammonium nitrate at high temperature. J Phys Chem. 1989;93:4029–33.
20. Oxley JC, Kauchik SM, Gilson NS. Thermal decomposition of ammonium nitrate-based composites. Thermochim Acta. 1989; 153:269–86.